Published in final edited form as:
Glia. 2013 February ; 61(2): 240–253. doi:10.1002/glia.22430.

The 4.1B cytoskeletal protein regulates the domain organization and sheath thickness of myelinated axons

Steven Einheber[*,1], **Patrice Maurel**[*,2], **Xiaosong Meng**[*,3], **Marina Rubin**[3,#], **Isabel Lam**[3,¶], **Narla Mohandas**[4], **Xiuli An**[4], **Peter Shrager**[5], **Joseph Kissil**[6], and **James L. Salzer**[3,7,‡]

[1]Hunter College School of Health Sciences, New York, NY

[2]Department of Biological Sciences, Rutgers University, Newark, NJ

[3]Smilow Neuroscience Program, New York University Langone Medical Center, New York, NY

[4]The New York Blood Center, New York

[5]Department of Neurobiology and Anatomy, University of Rochester School of Medicine, Jupiter, FL

[6]Department of Cancer Biology, Scripps Research Institute, Jupiter, FL

[7]Departments of Cell Biology and Neurology, New York University Langone Medical Center, New York, NY

Abstract

Myelinated axons are organized into specialized domains critical to their function in saltatory conduction, i.e. nodes, paranodes, juxtaparanodes, and internodes. Here, we describe the distribution and role of the 4.1B protein in this organization. 4.1B is expressed by neurons, and at lower levels by Schwann cells, which also robustly express 4.1G. Immunofluorescence and immuno-EM demonstrates 4.1B is expressed subjacent to the axon membrane in all domains except the nodes. Mice deficient in 4.1B have preserved paranodes, based on marker staining and EM in contrast to the juxtaparanodes, which are substantially affected in both the PNS and CNS. The juxtaparanodal defect is evident in developing and adult nerves and is neuron-autonomous based on myelinating cocultures in which wt Schwann cells were grown with 4.1B-deficient neurons. Despite the juxtaparanodal defect, nerve conduction velocity is unaffected. Preservation of paranodal markers in 4.1B deficient mice is associated with, but not dependent on an increase of 4.1R at the axonal paranodes. Loss of 4.1B in the axon is also associated with reduced levels of the internodal proteins, Necl-1 and Necl-2, and of alpha-2 spectrin. Mutant nerves are modestly hypermyelinated and have increased numbers of Schmidt-Lanterman incisures, increased expression of 4.1G, and express a residual, truncated isoform of 4.1B. These results demonstrate that 4.1B is a key cytoskeletal scaffold for axonal adhesion molecules expressed in the juxtaparanodal and internodal domains and, unexpectedly, that it regulates myelin sheath thickness.

Keywords

nodes of Ranvier; myelin; axons; paranodes; cytoskeleton

[‡]Correspondence: James.Salzer@NYUMC.org.
[*]These authors contributed equally to this study
[#]Current address: Department of Pediatrics, University of Rochester School of Medicine, Rochester, NY
[¶]Current address: Department of Molecular Biology, Sloan-Kettering Institute, New York

Introduction

Myelinated axons in the central nervous system (CNS) and peripheral nervous system (PNS) are organized into a series of distinct subdomains, i.e. nodes, paranodes, juxtaparanodes, and internodes. This organization is essential for effective saltatory conduction and for the long-term integrity of myelinated axons. Indeed, disrupted domain organization results in conduction block and is associated with axonal degeneration, a key contributor to the morbidity of dysmyelinating and demyelinating disorders (Scherer and Wrabetz 2008).

Significant progress has been made in elucidating the composition of these axonal domains in recent years (Salzer et al. 2008; Susuki and Rasband 2008). The nodal complex includes two axonal adhesion molecules, neurofascin 186 (NF186) and NrCAM, the ion channels $Na_V1.6$ and KCNQ/Q3, and a cytoskeletal scaffold of ankyrin G to which these proteins bind and which, in turn, is linked to βIV spectrin. Nodes are flanked by the paranodal junctions consisting of a complex of Caspr and contactin on the axon and NF155 on the apposed glial loops. The juxtaparanodes, which are adjacent to the paranodes just under the compact myelin sheath, contain TAG-1 on the glial membrane, a complex of TAG-1, Caspr 2 and Kv1 channels on the axon (Poliak et al. 2003; Traka et al. 2003), and other components (Ogawa et al. 2010). Finally, the internode domain contains a unique set of adhesion molecules, including the myelin-associated glycoprotein (MAG), enriched along the inner turn of the glial cell, and members of the Nectin-like (Necl) protein family, i.e. Necl-1 and Necl-2 on the axon and Necl-2 and Necl-4 on the glial membrane (Maurel et al. 2007; Spiegel et al. 2007).

Recent studies indicate that paranodes, juxtaparanodes, and internodes all contain the 4.1B cytoskeletal protein (Buttermore et al. 2011; Horresh et al. 2010; Ogawa et al. 2006; Ohara et al. 2000). 4.1B is a member of a protein family that includes 4.1G, 4.1R, 4.1O and 4.1N (Parra et al. 2004); these proteins serve as adapters that link a variety of transmembrane proteins, including neuronal adhesion molecules, to the actin/spectrin cytoskeleton (Horresh et al. 2010; Sun et al. 2002). 4.1B interacts directly with the cytoplasmic tail of Caspr and Caspr2 via the latters' FERM (4.1, ezrin, radixin, moesin) binding motifs (Denisenko-Nehrbass et al. 2003; Gollan et al. 2002). Similarly, the Necl proteins, also called the SynCams (Biederer 2006), contain a FERM-binding domain in their cytoplasmic tails that likely mediates interactions with 4.1 proteins (Hoy et al. 2009; Yang et al. 2011). Interactions between 4.1 proteins and adhesion molecules with FERM binding domains promote the domain organization of myelinated axons (Girault et al. 2003; Horresh et al. 2010; Ogawa et al. 2006). In particular, recent studies implicate 4.1B in establishing the integrity of the juxtaparanodal domain (Buttermore et al. 2011; Cifuentes-Diaz et al. 2011; Horresh et al. 2010), but differ on whether 4.1B also has an essential role in the paranodes.

In this study, we have characterized further the role of 4.1 family members in the domain organization of myelinated axons. We show 4.1B is highly expressed along the axonal internode whereas 4.1G is expressed by Schwann cells along the internode and in Schmidt-Lanterman incisures. As previously reported, mice deficient in 4.1B exhibit substantial defects in the expression of juxtaparanodal components. We also demonstrate that mutant peripheral nerves exhibit a significant reduction in the expression of internodal proteins, modest hypermyelination, and increased numbers of incisures. Defects in the paranodes are modest, potentially due to compensation from 4.1R, which is upregulated, and/or from the persistent expression of a truncated isoform of 4.1B in these knockout mice. Together, these data support the notion that 4.1 proteins, and 4.1B in particular, are important components of the cytoskeletal scaffold that maintain the integrity of the domains of myelinated axons.

Materials and methods

Mouse Genotyping

Generation of the 4.1B (*4.1B*$^{-/-}$) and 4.1R (*4.1R*$^{-/-}$) knockout mice have been described previously (Shi et al. 1999; Yi et al. 2005). In both cases, mice were backcrossed onto the C57BL/6 background. Mice were genotyped by PCR (Biorad Cycler, Hercules, CA) using the following primers: G2 (5′- CGC CAC CGT CTG AGC AGC -3′), G4 (5′- GCA CGT TTG GTA GCA GTT CCC -3′) and puro-1255 (5′- GCA CGA CCC CAT GCA TCG -3′). After an initial step of denaturation at 95°C for 3 min., PCR was carried out for 30 cycles at 94°C for 30 sec, 61°C for 30 sec, and 72°C for 1 min., and followed by a 10 min. extension at 72°C for 10 min. The expected 310 bp product for wild-type allele (G2/G4 primers) and 670 bp product for the mutant allele (G2/puro-1255 primers) were separated on a 1% agarose gel.

Tissue Culture Methods

Mouse dorsal root ganglia (DRG) were isolated from E14.5 embryos and established on collagen-coated 12 mm glass coverslips as previously described (Maurel et al. 2007), in neurobasal medium (Invitrogen, Carlsbad, CA) supplemented with B27 (Invitrogen), and 50 ng/ml NGF (Harlan, Bioproducts for Science). Cultures were cycled with fluoro-deoxyuridine and uridine (FdUR/U) (Sigma, St Louis, MO) for 10 days to eliminate non-neuronal cells, and then maintained another 6 days in absence of FdUR/U until DRG axons reached the periphery of the coverslips. Primary rat Schwann cells, prepared as previously described (Einheber et al. 1997), were added to purified DRG neurons (200,000 cells/coverslip) in Minimal Essential Medium (MEM) (Invitrogen) supplemented with 10% FBS, 0.4% glucose, 2 mM L-glutamine and 50 ng/ml NGF. After 3 days, myelination was initiated by supplementing the media with 50 μg/ml of ascorbic acid (Sigma-Aldrich), and cultures were maintained for 3 weeks.

Antibodies

Chicken polyclonal antibodies included the anti-MBP AB9348 and the anti-P0 AB9352 from Millipore (Temecula, CA), the anti-CADM1 (Necl-2) clone 3E1 (MBL International, Woburn, MA), and the anti-neurofilament PCK-593-P (Covance, Princeton, NJ). Rabbit polyclonal antibodies included anti-α1-actin A-2066 (Sigma, St. Louis, MO), anti-MAG Pep1 (Pedraza et al. 1990) and anti-peripherin antibody (gift of E. Ziff) and anti-ankyrin G (gift of S. Lux). Guinea pig polyconal antibodies included the anti-CASPR1 (gift from Manzoor Bhat, University of Texas, San Antonio), the anti-Necl-1 gp1733 and anti-Necl-4 gp1734 (Maurel et al. 2007). Mouse monoclonals included antibodies against MBP (SMI 94; Covance), pan sodium channel (Sigma), Kv1.1 (Alomone Labs), alpha II spectrin (Xu et al. 2001), ß-actin (clone AC-15; Sigma) were used. Antibodies against 4.1B, 4.1N, 4.1G and 4.1R including those to the head piece (HP) and to specific unique (U) domains, were described in our previous study (Kang et al. 2009a). Antibodies to 4.1B from Protein Express (Chiba, Japan) (Ohara et al. 2000) were also used. Secondary antibodies were IRDye-680CW-conjugated goat anti-rabbit and goat anti-mouse (LI-COR Biosciences, Lincoln, NE), IRDye-800CW-conjugated goat anti-chicken and goat anti-guinea pig (Rockland, Gilbertsville, PA), rhodamine-X-conjugated donkey anti–mouse and FITC-conjugated donkey anti–guinea pig (Jackson ImmunoResearch, West Grove, PA). Immunofluorescent preparations were examined by epifluorescence on a LSM 510 confocal microscope (Carl Zeiss MicroImaging, Inc.). Images were acquired with Neofluor 40x NA 1.3 oil or Apochromat 63x NA 1.4 oil objectives on an 8-bit photomultiplier tube using the LSM software. In some cases, brightness and contrast were adjusted with Photoshop 7.0 (Adobe).

Western blotting

Adult mice sciatic nerves from 3 separate paired littermates (WT vs. *4.1B*$^{-/-}$) were lysed in 150 mM NaCl, 25 mM Tris buffer pH 7.5, 1 % SDS, supplemented with a protease inhibitor cocktail (Roche, Branford, Ct) and Western blots were carried out as previously described (Maurel et al. 2007). Appropriate regions of the blots were cut and probed for MAG, MBP, P0, peripherin, α-actin, β-actin, αII spectrin and ankyrin G. To detect Necl-1, Necl-2 and Necl-4, lysates were first subjected to deglycosylation with PNGase F (New England Biolabs, Ipswich, MA) prior to SDS-PAGE fractionation (Maurel et al. 2007). Proteins were visualized with HR-conjugated or IRDye secondary antibodies; in the latter case, the intensity of the detected bands was quantified by measuring the integrated intensity (I.I.) using the Odyssey Imaging System (LI-COR Biosciences, Lincoln, NE). The percentage of change in protein level expression was measured as: (I.I.^{ko}/I.I.^{wt}) - 1) × 100.

Behavioral Studies

To study motor and exploratory behavior, mice were analyzed in open field tests as described previously with slight modifications (Bhat et al. 2001). Twenty adult wt and *4.1B*$^{-/-}$ mice (ten male and ten female for each) were tested. In brief, animals were placed in the center of a 33 cm × 56 cm grid with 6 cm × 6 cm squares surrounded by walls 32 cm high. Two observers recorded the number of gridlines crossed by the mice during a one-minute period. Counts obtained in three trials per mouse were averaged and analyzed statistically by the unpaired t-test. To measure motor coordination and fatigue, the same 20 wt and *4.1B*$^{-/-}$ mice were examined by the rotarod test. Prior to testing animals were trained on the rotarod (TSE Systems, Inc. model 7600, Bad Homburg, Germany) in three 30 sec sessions at 18 revolutions/sec, each separated by an interval of rest. After training, the length of time animals could remain on the rotarod at 18 revolutions/sec was measured over a maximum period of 120 seconds. Those animals that never fell off were given a score of 120 seconds. Three trials were performed for each animal and the times averaged. Measurements were analyzed statistically by unpaired t-test.

Electron Microscopy and Morphometry

Sciatic and optic nerves from wt and *4.1B*$^{-/-}$ mice were processed for electron microscopy as previously described (Einheber et al. 2006). In brief, animals were anesthetized with pentobarbital and perfused with 3.75% acrolein/2% paraformaldehyde in 0.1M phosphate buffer, pH 7.4; nerves were post-fixed in the same solution for 30 minutes and embedded in EMbed 812 (Electron Microscopy Sciences). Ultrathin sections (70 nm) of the nerves were cut, collected on copper grids and counterstained with 5% uranyl acetate and Reynold's lead citrate. Sections were examined on a Philips CM10 electron microscope (Eindhoven, The Netherlands). Digitized images of optic and sciatic nerve cross-sections were analyzed using the ImageJ software (NIH). G ratios were determined by dividing the diameter of the axon by that of the total fiber diameter from 789 wt and 621 mutant sciatic nerve fibers and ~ 1,000 optic nerve fibers; three animals per genotype were used.

Immunoelectron Microscopy

For ultrastructural localization of 4.1B, 40 μm vibratome sections from adult Sprague Dawley rats perfused with 3.75%acrolein/2% paraformaldehyde in 0.1M phosphate buffer, pH 7.4 were labeled with anti-4.1B antibody (Protein Express) diluted 1/500 in the presence of 0.035% Triton X-100 (Einheber et al. 1996). Bound primary antibody was detected using the avidin-biotin complex (ABC) peroxidase technique and the chromagen 3,3′ diaminobenzidine (Aldrich Chemical Co.). To determine the distribution of 4.1B in the corpus callosum, vibratome sections from acrolein/paraformaldehyde perfused wild type mice were incubated with an anti-4.1B antibody diluted 1/250 in 0.035% Triton X-100 and

then processed for silver-enhanced immunogold labeling as described (Einheber et al. 1997). Immunolabeled sections of sciatic nerve and brain were post-fixed in osmium tetroxide, dehydrated in a graded series of alcohols and embedded in EMbed 812. Ultrathin sections (70 nm) of the sciatic nerve or corpus callosum were cut and counterstained as described above.

Electrophysiology

Animals were euthanized by CO_2 inhalation and optic or sciatic nerves were dissected. Nerves were placed in a temperature controlled chamber and perfused with oxygenated Locke's solution containing (mM): NaCl 154, KCl 5.6, $CaCl_2$ 2, D-glucose 5, HEPES 10, pH 7.4. Each end of the nerve (or branch in the case of the sciatic nerve) was drawn into the tip of a suction electrode. Stimuli consisting of 50 μsec pulses were delivered to one electrode via a stimulus isolation unit. Compound action potentials (CAPs) were amplified, filtered at 10 kHz, digitized at 50-100 kHz, and analyzed on a laboratory computer. CAP peaks were analyzed by fitting to a third order polynomial and differentiating. Conduction velocity was calculated as the length of the nerve between the electrodes, divided by the time to the peak amplitude in the CAP. To record the small signals from unmyelinated C-fibers, typically 8-16 sweeps were averaged. To measure refractory period, pairs of stimuli were delivered, varying the duration between pulses (T). The ratio of the amplitude of the second response to that of the first was then calculated, and the refractory period was taken as the T for this ratio to reach 0.5 (measured by interpolation).

Results

4.1B is primarily expressed by neurons, 4.1G is specifically expressed by Schwann cells

We first examined the expression of all 4.1 proteins in DRG neurons and Schwann cells by immunofluorescence staining (Fig. 1). These studies demonstrated 4.1B is expressed by Schwann cells and robustly by neurons. Neurons also express 4.1N and 4.1R at levels that are detectable just above background. As previously reported (Ohno et al. 2006), Schwann cells express 4.1G at high levels. Western blotting data confirmed that Schwann cells express 4.1B and demonstrated that its expression is modestly upregulated by forskolin treatment (data not shown), which is known to promote a promyelinating Schwann cell phenotype (Morgan et al. 1991). These results indicate that 4.1B is expressed by both neurons and Schwann cells whereas 4.1G is specifically expressed by Schwann cells.

4.1B is expressed along the entire axon except at nodes of Ranvier

We next examined the expression of 4.1B, and other 4.1 proteins, in myelinated fibers by immunofluorescence. Sciatic nerves were fixed, teased and stained for various domain markers. As shown in Fig. 2A and B, staining with a previously described antibody (Ohara et al. 2000), 4.1B is detected at high levels along the entire length of myelinated nerve fibers, at all sites of axon-Schwann cell apposition except at the nodes of Ranvier. We did not observe an enrichment of 4.1B in the paranodes or juxtaparanodes with a variety of different anti-4.1B polyclonal antibodies. When nerves were fixed with 10% TCA, which we (Melendez-Vasquez et al. 2001) and others have used to stain cytoskeletal proteins in myelinated axon, we also detected 4.1B in the SLIs of Schwann cells (data not shown), suggesting the epitope identified by this antibody may be masked in the clefts. These results indicate that both neurons and Schwann cells express 4.1B. Staining for 4.1G demonstrated high-level expression along the internode and particularly in the SLIs (Fig. 8C). In agreement with the minimal expression of 4.1N and 4.1R by DRG neurons and Schwann cells (Fig. 1), these proteins were not detected in wt teased sciatic nerves (data not shown).

As the localization of 4.1B along the internode could reflect expression by axons, by Schwann cells, or both, we analyzed 4.1B expression further by immuno-EM. We stained sections of sciatic nerve and corpus callosum with the anti-4.1B antibody and either an HRP (Fig. 2Ca,b) or gold-conjugated secondary antibody (Fig. 2D, Ea,b). In both cases, 4.1B was detected subjacent to the axon membrane indicating expression along the internode is axonal. We also observed some expression of 4.1B at lower levels in Schmidt-Lanterman incisures (data not shown). In the CNS (i.e. the corpus callosum), expression of 4.1B was readily detectable along the myelinated internode and, in some cases, appeared to be enriched at paranodes (Fig. 2Eb). Specificity of the staining was underscored by the lack of immunogold labeling in preparations prepared from *4.1B*$^{-/-}$ mice (Fig. 2F); these mice are described further below.

Characterization of the *4.1B*$^{-/-}$ mice

Mice deficient in 4.1B have been reported previously (Yi et al. 2005). We confirmed that these mice are substantially deficient in 4.1B by Western blot analysis of brain lysates (Fig. 3C) and via immunofluorescence staining of sciatic (Fig. 3D) and optic nerves (data not shown), and via the aforementioned immuno-EM analysis (Fig. 2F) with the Protein Express 4.1B antibody. Western blot analysis also demonstrated a slight increase in the amounts of the nodal marker, NrCAM, whereas both Caspr and Caspr 2 were slightly decreased.

As previously reported (Yi et al. 2005), knockout mice have no overt phenotype. We found when these mice are suspended by their tails, they clasp their fore and hind limbs abnormally together and become stationary (Fig. 3A); this is in contrast to wild type mice, which continue to actively struggle. Formal neurological testing revealed knockout mice were less exploratory in an open field test ($p<0.05$) and were less stable on the rotorod test ($p<0.014$) (Fig. 3B).

We next investigated the effects of loss of 4.1B on the organization of myelinated axon domains in the PNS and CNS (Figs. 4, 5). As shown in Fig. 4A, both the nodes and paranodes were preserved based on staining with markers of nodes (sodium channels, βIV spectrin) and paranodes (Caspr); similar results were observed when nodes were stained for ankyrin G or NrCAM and paranodes were stained for contactin (data not shown). There were subtle changes in the mutant mice including slight widening of PNS nodes of Ranvier (i.e. 1.7 μm vs. 2 μm in the wt vs. *4.1B*$^{-/-}$ mice) and of the paranodes (4.5μm vs 4.9μm); axon diameter at these sites was not affected. In addition, the boundary between these domains was not always well delineated in the *4.1B*$^{-/-}$ vs. wt nerves, with some attenuation of Caspr expression at the paranodes (Fig. 4B, arrowhead), occasional intrusion of Caspr staining into the node, and some expression of NaChs in the paranode. Caspr staining in the juxtamesaxon along the internode was also frequently absent or disrupted in the knockout mice (Fig. 4B).

The most striking change in the knockout mice was the frequent loss of the juxtaparanodal domain in both the PNS and CNS as indicated by staining for Kv1.2 (Fig. 4B); other juxtaparanodal markers including Caspr2 and TAG1 were also markedly reduced (data not shown). This loss was fully evident at P16, the earliest time point examined in the PNS (data not shown). This defect was incomplete as a number of juxtaparanodes in the *4.1B*$^{-/-}$ nerves exhibited residual Kv1 channel expression. Interestingly, at higher magnification, staining for Kv1.2 was still detectable along the axon in what appeared to be intracellular vesicles (Fig. 4B). A comparable loss of the juxtaparanodes was also observed in the CNS as shown in staining of the optic nerves (Fig. 4C).

Because 4.1B is also expressed at lower levels by Schwann cells (Fig. 1), we examined whether the loss of the juxtaparanodes was due to the loss of its expression in axons,

Schwann cells, or potentially both. To this end, we cultured *4.1B*$^{-/-}$ or wild type mouse neurons with wild type rat Schwann cells under myelinating conditions and examined juxtaparanode formation. In general, juxtaparanodes formed normally when Schwann cells were cocultured with wild type neurons but not with the *4.1B*$^{-/-}$ neurons (Fig. 4D). In wild type neurons, Kv1.1 was concentrated at juxtaparanodes adjacent to both nodes (white arrowhead) and heminodes (yellow arrowhead). In contrast, in the *4.1B*$^{-/-}$ neurons, Kv1.1 expression was diffusely present along axons, with minimal enrichment in the juxtaparanodes. These results indicate that the localization of juxtaparanodal components depends upon the axonal expression of 4.1B.

We next examined the expression of the Necl proteins along the internodes and in the incisures. In the internodes of wild type mice, Necl-1 is expressed by axons, Necl-2 by both axons and Schwann cells, and Necl-4 by Schwann cells; all three Necls are present in the clefts of myelinating Schwann cells (Maurel et al. 2007; Spiegel et al. 2007) (Fig. 5A). By comparison, in the PNS and CNS of the *4.1B*$^{-/-}$ mice, there was a modest but significant reduction of Necl-1 and Necl-2 expression along the internodal membrane of the axon (Fig. 5A, C). Their expression in the clefts did not appear to be reduced in the knockout mice. In contrast, staining for Necl-4 along the glial internode and in the clefts was unchanged or slightly increased (Fig. 5). As 4.1 proteins are known to interact with spectrin proteins (Baines 2010), we also analyzed the expression of spectrin isoforms. We found the αII spectrin isoform to be highly expressed along the internode, suggestive of axonal expression. In the *4.1B*$^{-/-}$ nerves, expression along the internode was considerably reduced (Fig. 5B). These data implicate αII spectrin as a new component of the internodal, likely axonal cytoskeletal and strongly suggest it interacts with 4.1B.

To corroborate these staining results, we analyzed the expression of these and other components by Western blotting of lysates of sciatic nerves from wild type and *4.1B*$^{-/-}$ mice and quantified expression by LICOR analysis (Fig. 5D). These results confirm a substantial decrease in the expression of Necl-1, Necl-2, and alpha-II spectrin in the *4.1B*$^{-/-}$ mice. Interestingly, we also observed an increase in the expression of several other components including MAG, Necl-4 and alpha actin, which are all components of the Schmidt-Lanterman clefts. Components of compact myelin (P0 and MBP), and of the node (ankyrin G) were largely unaffected. Modest reductions in both beta actin and CNPase were also detected.

The ultrastructure of the myelinated sheath in nerves from *4.1B*$^{-/-}$ mice

We next investigated the ultrastructure of the myelin sheath of sciatic and optic nerves from *4.1B*$^{-/-}$ mice by electron microscopy. The organization of the myelin sheath appeared to be well preserved in both the PNS and CNS; myelin was compacted appropriately and of normal or slightly increased thickness (Fig. 6A). To more precisely characterize sheath thickness, we quantified axon diameters and *g* ratios, comparing sciatic nerves and optic nerves from wild type and *4.1B*$^{-/-}$ mice. Analysis of the diameters of myelinated axons (AD) in the PNS indicates there is an increase in the percentage of axons with small diameters that are myelinated (Fig. 6B). Additional analysis shows that the myelin sheath thickness is also increased in *4.1B*$^{-/-}$ nerves, with *g* ratios in sciatic nerves of 0.690 for wt vs. 0.663 for *4.1B*$^{-/-}$ mice ($p<0.0001$). This increase in myelin sheath thickness is evident at all axon diameters (Fig. 6C). Despite the increase in sheath thickness, the average internode length was unaffected or slightly shorter in the *4.1B*$^{-/-}$ mice (520 um for wt vs. 506 um for *4.1B*$^{-/-}$). G ratios in the optic nerves were essentially equivalent (0.828 for wt vs. 0.819 for *4.1B*$^{-/-}$ optic nerves).

We analyzed the ultrastructure of the nodal region in further detail (Fig. 7). The reduction in the diameter of the axon at nodes in the PNS was present in both wild type and knockout

nerves (Fig. 7A). In addition, at higher magnification, the periaxonal space i.e. the space between the axon and apposed Schwann cell membrane along the internode, did not appear to be affected (data not shown) despite the modest reduction in Necl-1 and -2 levels. The paranodal organization also appeared normal with the glial loops consistently attached to the axon and transverse bands present between the paranodal loops and the axon (Fig. 7A, B).

One structural change evident in the *4.1B*$^{-/-}$ nerves is a substantial increase in the numbers of Schmidt-Lanterman incisures. Analysis of the numbers of clefts indicates there is a more than 2 fold increase per unit length of the internode in the *4.1B*$^{-/-}$ nerves (Fig. 7C). This increase was apparent by immunofluorescence after staining for a number of cleft markers, including 4.1G (see below).

Persistence of a truncated 4.1B isoform and compensatory changes of 4.1 proteins

The preservation of the paranodal organization, in contrast to the juxtaparanodes, raised the possibility of compensation by other 4.1 proteins. We analyzed sciatic nerves from wild type and 4.1B$^{-/-}$ mice with an additional panel of antibodies directed against 4.1B, and with antibodies to other 4.1 family members (Kang et al. 2009a). Using these antibodies, we were able to detect some immunoreactivity of 4.1B in the nerves of the *4.1B*$^{-/-}$ mice by visual inspection and on images captured with prolonged exposure (inset, Fig. 8A). This low level staining was detected primarily in the clefts rather than along the axonal membrane suggesting persistent expression by Schwann cells.

In addition, we found 4.1R to be increased in the paranodes, although not elsewhere (Fig. 8B), in agreement with (Horresh et al. 2010). Expression of 4.1R was also modestly increased in the 4.1B$^{-/-}$ mice based on Western blot analysis (Fig. 8E) suggesting expression of 4.1R in the paranodes reflects both increased expression and redistribution. 4.1G was also upregulated, consistent with the increase in cleft numbers, whereas 4.1N appeared to be unchanged on Western blots (Fig. 8E).

The increased expression of 4.1R in the paranodes suggested it might contribute to the relative preservation of the paranodes. To test this possibility, we generated 4.1B/4.1R double knockout mice. These mice were born at sub-Mendelian ratios (~ 1:100 rather than the expected ratio of 1:16) consistent with earlier reports that 4.1R nulls are also born at sub-Mendelian ratios (Kang et al. 2009b). The mice appeared slightly smaller in size than the *4.1B*$^{-/-}$ mice but were not noticeably more neurologically impaired. Importantly, Caspr was still expressed in the paranodes suggesting that the preservation of the paranodes observed in these mice is not dependent on the upregulation of 4.1R (Fig. 8D).

Nerve conduction is not affected in the 4.1B deficient mice

Finally, we investigated the electrophysiological properties of optic and sciatic nerves from wt and *4.1B*$^{-/-}$ mice. The fast peak in the compound action potential from sciatic nerves represents the contribution from myelinated axons. The nerve conduction velocity (NCV) from these fibers was unaffected by the deletion of 4.1B (Fig. 9A). Similarly, there was no significant decrease in the NCVs in unmyelinated C fibers of the sciatic nerve (Fig. 9B) or optic nerves (Fig. 9D) of *4.1B*$^{-/-}$ mice. The refractory period was measured in sciatic nerves and was also found to be unchanged in the null animal (Fig. 9C). Optic nerve action potentials are sensitive to K^+ channel block by 4-aminopyridine (4-AP). Fig 9E shows sweeps from a wt animal before and after exposure to 1 mM 4-AP (upper records). The CAP is much larger and broader with the drug. The lower sweeps show records from a *4.1B*$^{-/-}$ mouse. Despite the loss of juxtaparanodal elements, including clustered voltage-dependent K^+ channels, the CAP responds similarly to 4-AP as in the wild type.

Discussion

We have shown that 4.1B is a major component of the axonal membrane cytoskeleton and likely tethers adhesion complexes in all domains of myelinated axons except at the node of Ranvier. This is most evident at the juxtaparanodes, where 4.1B is required in a neuron-autonomous fashion, and along the internodes for full expression of Necl-1 and -2. We also show that despite the loss of 4.1B, there was relative preservation of the paranodal domain. Finally, there is an increase in myelin sheath thickness and of cleft numbers in *4.1B*$^{-/-}$ mice. These findings are considered further below.

Our studies corroborate that 4.1B comprises a major component of the cytoskeletal complex of myelinated axons at all sites except at the node of Ranvier in accord with recent reports (Buttermore et al. 2011; Cifuentes-Diaz et al. 2011; Horresh et al. 2010). Prior to myelination, 4.1B is diffusely expressed along the entire axon (Fig. 1). With myelination, 4.1B continues to be expressed along most of the axon, except at nodes, where it co-localizes with distinct sets of axonal adhesion molecules with cytoplasmic FERM-binding motifs; these include Caspr at the paranodes, Caspr 2 at the juxtaparanodes, and the Necls along the internode. Interestingly, 4.1B persists at the paranodes of Caspr null mice (Horresh et al. 2010); this may be due to compensation by Caspr 2, which is expressed at this site in the Caspr nulls. The absence of 4.1B at the node may reflect the lack of 4.1-binding proteins at this site – such proteins may be required for either targeting and/or stable expression of 4.1B. Alternatively, 4.1B may be actively excluded from the node by the physical presence of the distinctive nodal cytoskeleton (Susuki and Rasband 2008).

The loss of the juxtaparanodes in the absence of 4.1B agrees with several recent reports (Buttermore et al. 2011; Cifuentes-Diaz et al. 2011; Horresh et al. 2010). The defect in the juxtaparanodes was fully evident at P16, the earliest time examined, and persists into adulthood in both the PNS and CNS, suggesting that 4.1B is required to establish this domain. In agreement with a direct role of 4.1B in organizing the juxtaparanodal complex on axons, loss of the juxtaparanodes was neuron-autonomous (Fig. 4D). Caspr 2 on the axon is know to interact with 4.1B at this site (Denisenko-Nehrbass et al. 2003); such interactions likely stabilize Caspr 2 expression (Horresh et al. 2008) and may promote its trafficking to the plasma membrane, akin to other 4.1B-binding proteins (Kang et al. 2009a). In turn, Caspr 2 is required for the clustering of Kv1 channels at the juxtaparanodes (Poliak et al. 2003). Interestingly, some of the residual staining of Kv1.1 and 1.2 in the *4.1B*$^{-/-}$ mice appears to be vesicular (Fig. 4B), possibly reflecting internalization due to failure of Kv1 to be stabilized by a Caspr2/4.1B complex. Indeed, Caspr2 is internalized via a juxtamembrane sequence that overlaps with its FERM-binding domain (Bel et al. 2009) suggesting binding to 4.1B may preclude its clearance.

Despite the loss of the juxtaparanodes, we were unable to identify any significant defect in the electrophysiological properties of sciatic or optic nerves from the *4.1B*$^{-/-}$ mice (Fig. 8). The minimal electrophysiological consequences of the loss of the juxtaparanodes in these mice are similar to findings in mice in which individual Kv1 channels are deficient (Zhou et al. 1998) or the juxtaparanodes are deficient, i.e. in the Caspr2 or TAG-1 knockouts (Poliak et al. 2003). The preservation of PNS function in these mice also raises the possibility that their modest neurological deficits of the *4.1B*$^{-/-}$ mice reflect expression and the potential function of 4.1B within the CNS. Action potentials in PNS axons are sensitive to 4-AP block early in development, when Kv1 channels are not yet sequestered in the juxtaparanodes, but become almost entirely unresponsive to the drug in the adult (Vabnick et al. 1999). In contrast, the CAP in wild type optic nerves is significantly increased in amplitude and is broadened by 4-AP. We show here that this sensitivity of the CNS to K+ channel block remains persists in the *4.1B*$^{-/-}$ mice despite the lack of juxtaparanodal clustering of Kv1

channels. KCNQ2/3 channels, present at many CNS nodes, are not blocked by this drug (Devaux et al. 2004). Further, 4-AP broadening of the CAP remains following deletion of Kv3.1b channels, also nodal in the CNS (Devaux et al. 2003). Thus, it is likely that another, as yet unidentified K+ channel type, is present in CNS axons and plays an important role in excitability.

We also demonstrate that the Necl-1 and -2, but not Necl-4, are reduced along the internode (Fig. 5). The reductions in the levels of Necl-1 and -2, which were significant but incomplete (Fig. 5), are consistent with the known interaction of the Necls with 4.1 family members, including 4.1B (Hoy et al. 2009; Yang et al. 2011). Interestingly, Necl-4 levels along the Schwann cell internode were normal despite substantial reduction of its cognate, axonal ligand (Necl-1). These findings indicate that Necl-4 levels are not dependent on *trans* interactions with its ligand. Rather, Necl-4 levels appear to be highly dependent on cytoplasmic interactions with 4.1G [(Ivanovic et al. 2012) and X. Meng, J. Salzer, unpublished] in the Schwann cell.

We have also identified αII spectrin as a component of the internodal cytoskeleton and show that its expression at this site depends, in part, on 4.1B (Fig. 5). This spectrin isoform was previously described as a component of the node and paranodes in zebrafish (Voas et al. 2007) and, together with βII spectrin, was found to be enriched in the mammalian paranodes (Ogawa et al. 2006). While we also observed αII expression in the paranodes, its expression is much broader being present along the entire internode (Fig. 5) consistent with a direct interaction with 4.1B. A recent report also identifies αII and βII spectrins as present in Schwann cells (Susuki et al. 2011). Potentially, differences between various αII antibodies may account for an apparent discrepancy with previous reports on its localization. As α and βII spectrins are frequently associated (Baines 2010), we expected to also find the latter enriched along the internode as well. Although our initial staining results were inconclusive, βII spectrin was indeed reported to be enriched along the internode and to be substantially reduced in *4.1B*$^{-/-}$ mice (Cifuentes-Diaz et al. 2011).

There is surprising preservation of the paranodes in the *4.1B*$^{-/-}$ mice, including persistence of the transverse bands (Fig. 7B). However, the organization of the paranodes was not fully normal as evidenced by patchy Caspr staining and occasional intrusion of nodal components into the paranodes. The relative preservation of the paranodes observed here agrees with that of Horresh et al. (2010) but contrasts with two recent reports, which used other knockout mice (Buttermore et al. 2011; Cifuentes-Diaz et al. 2011). We have detected a truncated (~ 60 kD) form of 4.1B in nerves of these mice (see Fig. 8E), as we previously reported in other tissues (Kang et al. 2009a). Although the precise structure of this residual 4.1B protein is not known, it cross-reacts with antibodies to both the head-piece (i.e. the U1 domain) and may contain a portion of the FERM motif. This truncated 4.1B protein could, in principle, contribute to the stability of the paranodes. However, by immunostaining, much of this persistent 4.1B immunoreactivity was detected at low levels in the clefts rather than in the paranodes (Fig. 8A, inset). This localization suggests it is expressed by Schwann cells rather than axons and may not significantly contribute to the stability of the paranodes. We have also detected 4.1B in wild type nerves in the clefts with acidic fixation methods and by immuno-EM (data not shown).

We have also found that 4.1R is modestly upregulated in the absence of 4.1B, in agreement with one report (Horresh et al. 2010) but not another (Buttermore et al. 2011). Potentially, upregulation of 4.1R expression may contribute to the preserved paranode organization. In our initial analysis of the 4.1R/4.1B double knockout, Caspr expression persists even in the absence of both 4.1 proteins (inset, Fig. 8D). Additional studies will be required to

determine if the transverse bands are impaired in the double nulls compared to the *4.1B*$^{-/-}$ mice.

In addition to these changes in the domain organization of the *4.1B*$^{-/-}$ mice, we also observed an increase in the numbers of smaller diametered axons that are myelinated (Fig. 6B) and a modest increase in myelin sheath thickness at all fiber diameters (Fig. 6C). The modest reduction in axon diameters was also recently observed in a different 4.1B null mouse and may reflect a loss of spectrins along the internode reported here and elsewhere (Cifuentes-Diaz et al. 2011). A reduction in axon caliber could contribute to a relative decrease in g ratios. However, myelin sheath thickness was increased around fibers of all diameters suggesting a more general hypermyelination effect. The mechanism(s) responsible for this increase in myelin thickness is not known. Potentially, changes in the level of adhesion molecules on the axon and Schwann cell surface might be promyelinating or, alternatively, 4.1B deficiency might affect levels of growth factors important for myelination. One such candidate is type III neuregulin, the major promyelinating signal identified to date on axons which, when overexpressed, results in hypermyelination (Nave and Salzer 2006). However, expression of neuregulin in neurons was unchanged in the *4.1B*$^{-/-}$ mice (X. Meng, J. Salzer, unpublished) suggesting other mechanisms, still to be determined, are responsible. Interestingly, the increase in myelin sheath thickness was not associated with longer internodes. Rather there was a trend to shorter internodes, also observed in another 4.1B mutant mouse (Cifuentes-Diaz et al. 2011).

The sciatic nerves of the *4.1B*$^{-/-}$ mice also have more Schmidt-Lanterman incisures than wild type mice (Fig. 8C; quantitated in Fig. 7C), consistent with the increased expression of the cleft components, MAG, Necl-4, and actin (Fig. 5). A comparable increase in clefts was recently reported in another 4.1B knockout mouse (Cifuentes-Diaz et al. 2011). The mechanisms responsible for the increase in cleft numbers remain to be established. As reported previously (Ghabriel and Allt 1981), there are more clefts in larger diameter nerve fibers (Fig. 7C). However, the increase in clefts in the *4.1B*$^{-/-}$ mice is much greater than the modest increase in myelin thickness in these nerves. Loss of 4.1B may result in compensatory changes in the Schwann cell, including an increase in 4.1G (Fig. 8C). Further studies will be necessary to delineate the precise mechanisms involved.

Thus, we have shown that a 4.1B/spectrin II cytoskeletal complex supports the organization of myelinated axons, stabilizing the expression of multiple FERM-binding adhesion molecules in all axonal domains except at the node. The localization of 4.1G suggests that it has a complementary role in the organization of Schwann cell domains (Ivanovic et al. 2012). Other 4.1 family members are also important in the organization of myelinating Schwann cells including the ERM proteins, i.e. ezrin, radixin, moesin, in the nodal microvilli (Melendez-Vasquez et al. 2001; Scherer et al. 2001) and merlin (Denisenko et al. 2008). Together, these results implicate the 4.1 superfamily as key cytoskeletal components that promote the organization of the polarized domains of axons and myelinating Schwann cells.

Acknowledgments

We thank E. Peles, S. Lux, M. Bhat, M. Rasband for generously providing antibodies, Moses Chao for use of his imaging microscope, and Teresa Milner for advice and help with electron microscopy. This research was supported by grants from the NIH (NS043474, DK32094, and NS17965) and the National Multiple Sclerosis Society (RG 3985-A-11).

REFERENCES

Baines AJ. Evolution of the spectrin-based membrane skeleton. Transfus Clin Biol. 2010; 17:95–103. [PubMed: 20688550]

Bel C, Oguievetskaia K, Pitaval C, Goutebroze L, Faivre-Sarrailh C. Axonal targeting of Caspr2 in hippocampal neurons via selective somatodendritic endocytosis. J Cell Sci. 2009; 122:3403–13. [PubMed: 19706678]

Bhat MA, Rios JC, Lu Y, Garcia-Fresco GP, Ching W, St Martin M, Li J, Einheber S, Chesler M, Rosenbluth J. Axon-glia interactions and the domain organization of myelinated axons requires neurexin IV/Caspr/Paranodin. Neuron. 2001; 30:369–83. others. [PubMed: 11395000]

Biederer T. Bioinformatic characterization of the SynCAM family of immunoglobulin-like domain-containing adhesion molecules. Genomics. 2006; 87:139–50. [PubMed: 16311015]

Buttermore ED, Dupree JL, Cheng J, An X, Tessarollo L, Bhat MA. The cytoskeletal adaptor protein band 4.1B is required for the maintenance of paranodal axoglial septate junctions in myelinated axons. The Journal of neuroscience: the official journal of the Society for Neuroscience. 2011; 31:8013–24. [PubMed: 21632923]

Cifuentes-Diaz C, Chareyre F, Garcia M, Devaux J, Carnaud M, Levasseur G, Niwa-Kawakita M, Harroch S, Girault JA, Giovannini M. Protein 4.1B contributes to the organization of peripheral myelinated axons. PloS one. 2011; 6:e25043. others. [PubMed: 21966409]

Denisenko N, Cifuentes-Diaz C, Irinopoulou T, Carnaud M, Benoit E, Niwa-Kawakita M, Chareyre F, Giovannini M, Girault JA, Goutebroze L. Tumor suppressor schwannomin/merlin is critical for the organization of Schwann cell contacts in peripheral nerves. J Neurosci. 2008; 28:10472–81. [PubMed: 18923024]

Denisenko-Nehrbass N, Oguievetskaia K, Goutebroze L, Galvez T, Yamakawa H, Ohara O, Carnaud M, Girault JA. Protein 4.1B associates with both Caspr/paranodin and Caspr2 at paranodes and juxtaparanodes of myelinated fibres. Eur J Neurosci. 2003; 17:411–6. [PubMed: 12542678]

Devaux J, Alcaraz G, Grinspan J, Bennett V, Joho R, Crest M, Scherer SS. Kv3.1b is a novel component of CNS nodes. J Neurosci. 2003; 23:4509–18. [PubMed: 12805291]

Devaux JJ, Kleopa KA, Cooper EC, Scherer SS. KCNQ2 is a nodal K+ channel. J Neurosci. 2004; 24:1236–44. [PubMed: 14762142]

Einheber S, Bhat MA, Salzer JL. Disrupted axo-glial junctions result in accumulation of abnormal mtochondria at nodes of Ranvier. Neuron Glia Biol. 2006; 2:165–174. [PubMed: 17460780]

Einheber S, Schnapp LM, Salzer JL, Cappiello ZB, Milner TA. Regional and ultrastructural distribution of the alpha 8 integrin subunit in developing and adult rat brain suggests a role in synaptic function. J Comp Neurol. 1996; 370:105–34. [PubMed: 8797161]

Einheber S, Zanazzi G, Ching W, Scherer S, Milner TA, Peles E, Salzer JL. The axonal membrane protein Caspr, a homologue of neurexin IV, is a component of the septate-like paranodal junctions that assemble during myelination. J Cell Biol. 1997; 139:1495–1506. [PubMed: 9396755]

Ghabriel MN, Allt G. Incisures of Schmidt-Lanterman. Prog Neurobiol. 1981; 17:25–58. [PubMed: 7323300]

Girault JA, Oguievetskaia K, Carnaud M, Denisenko-Nehrbass N, Goutebroze L. Transmembrane scaffolding proteins in the formation and stability of nodes of Ranvier. Biol Cell. 2003; 95:447–52. [PubMed: 14597262]

Gollan L, Sabanay H, Poliak S, Berglund EO, Ranscht B, Peles E. Retention of a cell adhesion complex at the paranodal junction requires the cytoplasmic region of Caspr. J Cell Biol. 2002; 157:1247–56. [PubMed: 12082082]

Horresh I, Bar V, Kissil JL, Peles E. Organization of myelinated axons by Caspr and Caspr2 requires the cytoskeletal adapter protein 4.1B. J Neurosci. 2010; 30:2480–9. [PubMed: 20164332]

Horresh I, Poliak S, Grant S, Bredt D, Rasband MN, Peles E. Multiple molecular interactions determine the clustering of Caspr2 and Kv1 channels in myelinated axons. J Neurosci. 2008; 28:14213–22. [PubMed: 19109503]

Hoy JL, Constable JR, Vicini S, Fu Z, Washbourne P. SynCAM1 recruits NMDA receptors via protein 4.1B. Molecular and cellular neurosciences. 2009; 42:466–83. [PubMed: 19796685]

Ivanovic A, Horresh I, Golan N, Spiegel I, Sabanay H, Frechter S, Ohno S, Terada N, Mobius W, Rosenbluth J. The cytoskeletal adapter protein 4.1G organizes the internodes in peripheral myelinated nerves. The Journal of cell biology. 2012; 196:337–44. others. [PubMed: 22291039]

Kang Q, Wang T, Zhang H, Mohandas N, An X. A Golgi-associated protein 4.1B variant is required for assimilation of proteins in the membrane. J Cell Sci. 2009a; 122:1091–9. [PubMed: 19299464]

Kang Q, Yu Y, Pei X, Hughes R, Heck S, Zhang X, Guo X, Halverson G, Mohandas N, An X. Cytoskeletal protein 4.1R negatively regulates T-cell activation by inhibiting the phosphorylation of LAT. Blood. 2009b; 113:6128–37. [PubMed: 19190245]

Maurel P, Einheber S, Galinska J, Thaker P, Lam I, Rubin MB, Scherer SS, Murakami Y, Gutmann DH, Salzer JL. Nectin-like proteins mediate axon Schwann cell interactions along the internode and are essential for myelination. J Cell Biol. 2007; 178:861–74. [PubMed: 17724124]

Melendez-Vasquez CV, Rios JC, Zanazzi G, Lambert S, Bretscher A, Salzer JL. Nodes of Ranvier form in association with ezrin-radixin-moesin (ERM)-positive Schwann cell processes. Proc Natl Acad Sci U S A. 2001; 98:1235–1240. [PubMed: 11158623]

Morgan L, Jessen KR, Mirsky R. The effects of cAMP on differentiation of cultured Schwann cells: progression from an early phenotype (04+) to a myelin phenotype (P0+, GFAP-, N-CAM-, NGF-receptor-) depends on growth inhibition. J Cell Biol. 1991; 112:457–67. [PubMed: 1704008]

Nave KA, Salzer JL. Axonal regulation of myelination by neuregulin 1. Curr Opin Neurobiol. 2006; 16:492–500. [PubMed: 16962312]

Ogawa Y, Oses-Prieto J, Kim MY, Horresh I, Peles E, Burlingame AL, Trimmer JS, Meijer D, Rasband MN. ADAM22, a Kv1 channel-interacting protein, recruits membrane-associated guanylate kinases to juxtaparanodes of myelinated axons. J Neurosci. 2010; 30:1038–48. [PubMed: 20089912]

Ogawa Y, Schafer DP, Horresh I, Bar V, Hales K, Yang Y, Susuki K, Peles E, Stankewich MC, Rasband MN. Spectrins and ankyrinB constitute a specialized paranodal cytoskeleton. J Neurosci. 2006; 26:5230–9. [PubMed: 16687515]

Ohara R, Yamakawa H, Nakayama M, Ohara O. Type II brain 4.1 (4.1B/KIAA0987), a member of the protein 4.1 family, is localized to neuronal paranodes. Brain Res Mol Brain Res. 2000; 85:41–52. [PubMed: 11146105]

Ohno N, Terada N, Yamakawa H, Komada M, Ohara O, Trapp BD, Ohno S. Expression of protein 4.1G in Schwann cells of the peripheral nervous system. J Neurosci Res. 2006; 84:568–77. [PubMed: 16752423]

Parra M, Gee S, Chan N, Ryaboy D, Dubchak I, Mohandas N, Gascard PD, Conboy JG. Differential domain evolution and complex RNA processing in a family of paralogous EPB41 (protein 4.1) genes facilitate expression of diverse tissue-specific isoforms. Genomics. 2004; 84:637–46. [PubMed: 15475241]

Pedraza L, Owens GC, Green LA, Salzer JL. The myelin-associated glycoproteins: membrane disposition, evidence of a novel disulfide linkage between immunoglobulin-like domains, and posttranslational palmitylation. J Cell Biol. 1990; 111:2651–61. [PubMed: 1703542]

Poliak S, Salomon D, Elhanany H, Sabanay H, Kiernan B, Pevny L, Stewart CL, Xu X, Chiu SY, Shrager P. Juxtaparanodal clustering of Shaker-like K+ channels in myelinated axons depends on Caspr2 and TAG-1. J Cell Biol. 2003 others.

Salzer JL, Brophy PJ, Peles E. Molecular domains of myelinated axons in the peripheral nervous system. Glia. 2008; 56:1532–40. [PubMed: 18803321]

Scherer SS, Wrabetz L. Molecular mechanisms of inherited demyelinating neuropathies. Glia. 2008; 56:1578–89. [PubMed: 18803325]

Scherer SS, Xu T, Crino P, Arroyo EJ, Gutmann DH. Ezrin, radixin, and moesin are components of Schwann cell microvilli. J Neurosci Res. 2001; 65:150–64. [PubMed: 11438984]

Shi ZT, Afzal V, Coller B, Patel D, Chasis JA, Parra M, Lee G, Paszty C, Stevens M, Walensky L. Protein 4.1R-deficient mice are viable but have erythroid membrane skeleton abnormalities. J Clin Invest. 1999; 103:331–40. others. [PubMed: 9927493]

Spiegel I, Adamsky K, Eshed Y, Milo R, Sabanay H, Sarig-Nadir O, Horresh I, Scherer SS, Rasband MN, Peles E. A central role for Necl4 (SynCAM4) in Schwann cell-axon interaction and myelination. Nat Neurosci. 2007; 10:861–9. [PubMed: 17558405]

Sun CX, Robb VA, Gutmann DH. Protein 4.1 tumor suppressors: getting a FERM grip on growth regulation. J Cell Sci. 2002; 115:3991–4000. [PubMed: 12356905]

Susuki K, Raphael AR, Ogawa Y, Stankewich MC, Peles E, Talbot WS, Rasband MN. Schwann cell spectrins modulate peripheral nerve myelination. Proceedings of the National Academy of Sciences of the United States of America. 2011

Susuki K, Rasband MN. Spectrin and ankyrin-based cytoskeletons at polarized domains in myelinated axons. Exp Biol Med (Maywood). 2008; 233:394–400. [PubMed: 18367627]

Traka M, Goutebroze L, Denisenko N, Bessa M, Nifli A, Havaki S, Iwakura Y, Fukamauchi F, Watanabe K, Soliven B. Association of TAG-1 with Caspr2 is essential for the molecular organization of juxtaparanodal regions of myelinated fibers. J Cell Biol. 2003; 162:1161–72. others. [PubMed: 12975355]

Vabnick I, Trimmer JS, Schwarz TL, Levinson SR, Risal D, Shrager P. Dynamic potassium channel distributions during axonal development prevent aberrant firing patterns. J Neurosci. 1999; 19:747–58. [PubMed: 9880595]

Voas MG, Lyons DA, Naylor SG, Arana N, Rasband MN, Talbot WS. alphaII-spectrin is essential for assembly of the nodes of Ranvier in myelinated axons. Curr Biol. 2007; 17:562–8. [PubMed: 17331725]

Xu J, Ziemnicka D, Scalia J, Kotula L. Monoclonal antibodies to alphaI spectrin Src homology 3 domain associate with macropinocytic vesicles in nonerythroid cells. Brain Res. 2001; 898:171–7. [PubMed: 11292462]

Yang S, Weng H, Chen L, Guo X, Parra M, Conboy J, Debnath G, Lambert AJ, Peters LL, Baines AJ. Lack of protein 4.1G causes altered expression and localization of the cell adhesion molecule nectin-like 4 in testis and can cause male infertility. Molecular and cellular biology. 2011; 31:2276–86. others. [PubMed: 21482674]

Yi C, McCarty JH, Troutman SA, Eckman MS, Bronson RT, Kissil JL. Loss of the putative tumor suppressor band 4.1B/Dal1 gene is dispensable for normal development and does not predispose to cancer. Mol Cell Biol. 2005; 25:10052–9. [PubMed: 16260618]

Zhou L, Zhang CL, Messing A, Chiu SY. Temperature-sensitive neuromuscular transmission in Kv1.1 null mice: role of potassium channels under the myelin sheath in young nerves. J Neurosci. 1998; 18:7200–15. [PubMed: 9736643]

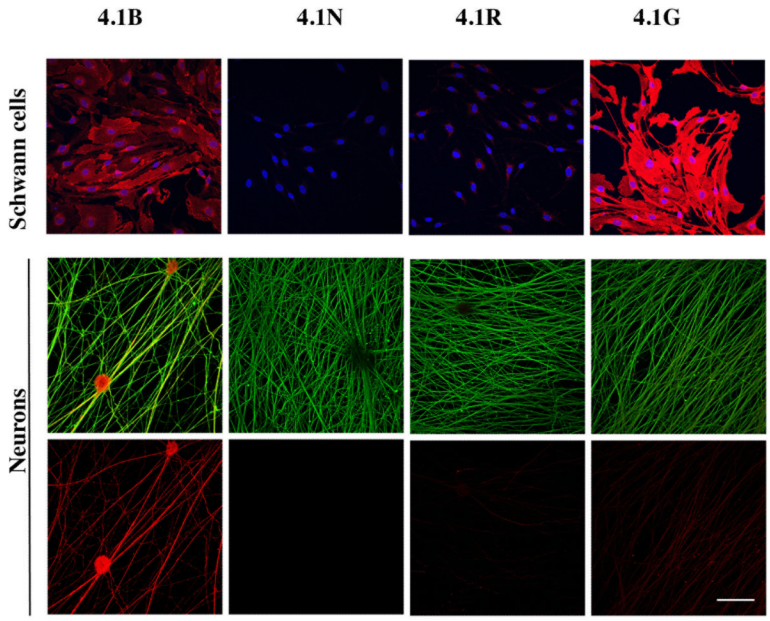

Figure 1. Expression of 4.1 proteins by neurons and Schwann cells

Immunostaining of Schwann cell and DRG neuron cultures for different members of the 4.1 family is shown. Schwann cells (top row) were double stained with Hoechst (blue) to demonstrate cell nuclei and for 4.1 proteins (red). Neurons (middle and bottom rows) were double stained for neurofilament (green) and 4.1 proteins (red) in the middle row and 4.1 proteins only, in the bottom row. Schwann cells express 4.1B at moderate levels and 4.1G at robust levels; neurons principally express 4.1B. Scale bars: panels A and B, 5 μm; panels C-F, 0.5 μm; bar 50 μm.

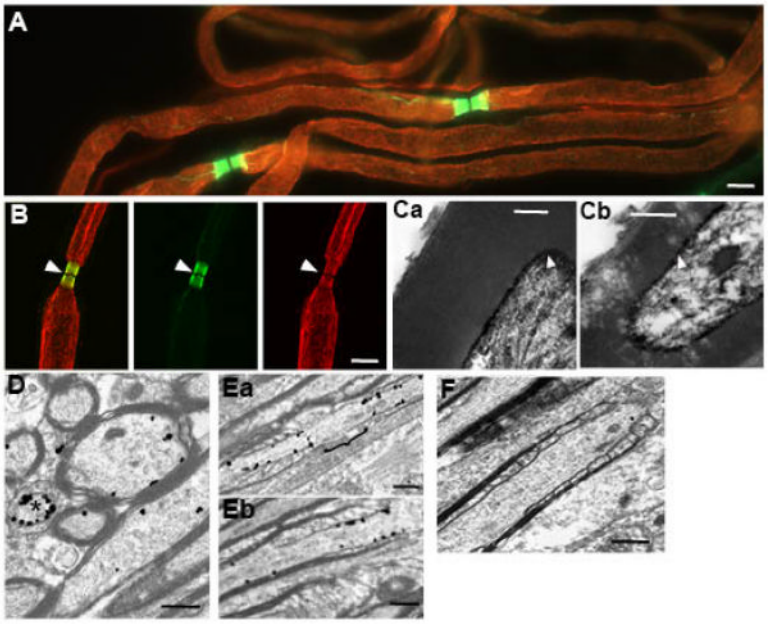

Figure 2. 4.1B is expressed along the axonal internode

A. Teased sciatic nerves stained for Caspr (green) and 4.1B (red) are shown in this confocal projection image. B. Higher power image of the paranodal region shows staining for 4.1B is concentrated along the membrane throughout the axon except for a small gap at the node (arrowheads). C. Immuno-peroxidase labeling of sciatic nerve sections demonstrates 4.1B is expressed along the axonal membrane (arrowheads). D. Immuno-EM of transverse sections of the corpus callosum demonstrates immuno-gold labeling of 4.1B along the internode of myelinated axons; fiber marked by an asterisk is sectioned through the paranode and demonstrates increased 4.1B expression, E. Longitudinal sections of the corpus callosum demonstrate increased expression in the paranodes with exclusion from the node of Ranvier (indicated with a brace); F. Few immungold particles were observed in sections of the corpus callosum from *4.1B*$^{-/-}$ mice.

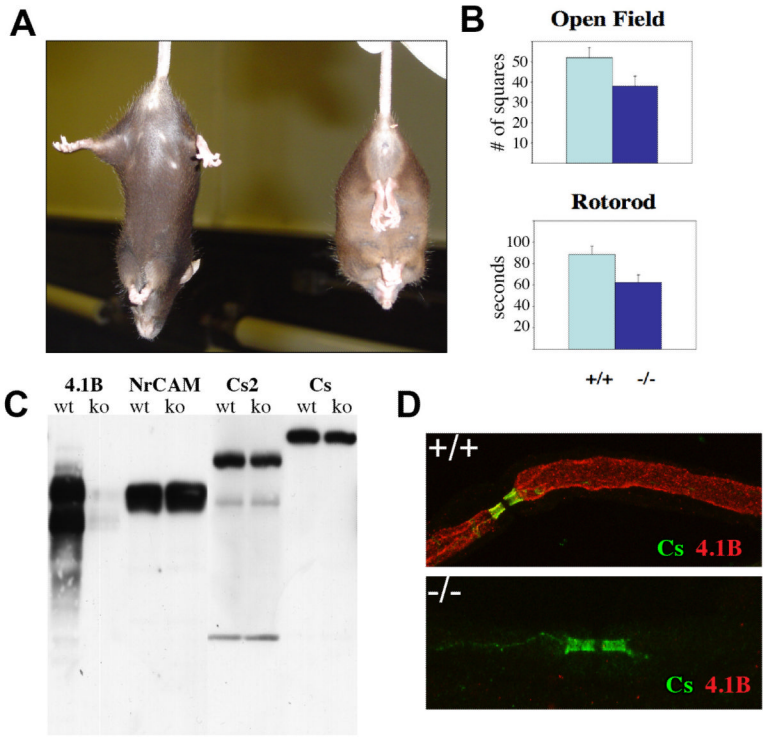

Figure 3. Characterization of the *4.1B*$^{-/-}$ mice

A) Wild type (left) and *4.1B*$^{-/-}$ mouse (right) are shown; *4.1B*$^{-/-}$ mice adopt a distinctive posture with their front and hind limbs clasped together when held by the tail. B) *4.1B*$^{-/-}$ mice exhibit statistically significant deficits in open field and rotorod tests. C) Western blot analysis of brain lysates demonstrated complete absence of 4.1B protein isoforms; a slight increase in NrCAM and a slight decrease in Caspr and Caspr 2 expression were also observed. D) Immunofluorescence staining of teased sciatic nerves showed loss of 4.1B expression along the internode; Caspr staining was relatively well preserved in the example shown.

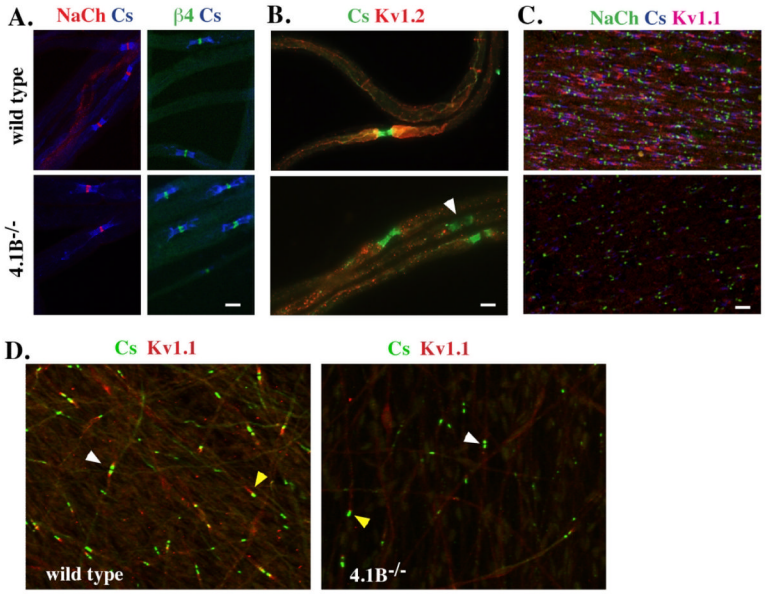

Figure 4. Organization of nodal region domains in the absence of 4.1B

Teased sciatic nerves from wild type and *4.1B*$^{-/-}$ mice were analyzed for the expression of nodal, paranodal and juxtaparanodal markers. A) Nodal, i.e. sodium channels and βIV spectrin, and a paranodal marker, i.e. Caspr, were largely unaffected in the knockouts although nodes were slightly wider and the paranodal and juxtamesaxonal staining of Caspr was attenuated. B) Kv1.2 (red) expression in the juxtaparanodes was frequently absent in the knockout nerves with punctate staining along the internode. An example of attenuated Caspr (green) staining is indicated (white arrowhead); the node just below exhibits a wider gap between the flanking, Caspr-positive paranodes. C. Loss of juxtaparanodal staining of Kv1.1 (red) was also observed in the optic nerve; sodium channel (green) and Caspr (blue) are also shown. D. Loss of the juxtaparanodes is neuron-autonomous. Neurons from wild type or *4.1B*$^{-/-}$ littermates were cocultured with wild type Schwann cells under myelinating conditions for two weeks and stained for Caspr (green) and Kv1.1 (red). Juxtaparanodes were present in the wild type but rare in the knockout cocultures; examples of nodes (white arrowheads) and heminodes (yellow arrowheads) are indicated. Scale bars: 10 μm (A), 5 μm (B), 5 μm (C).

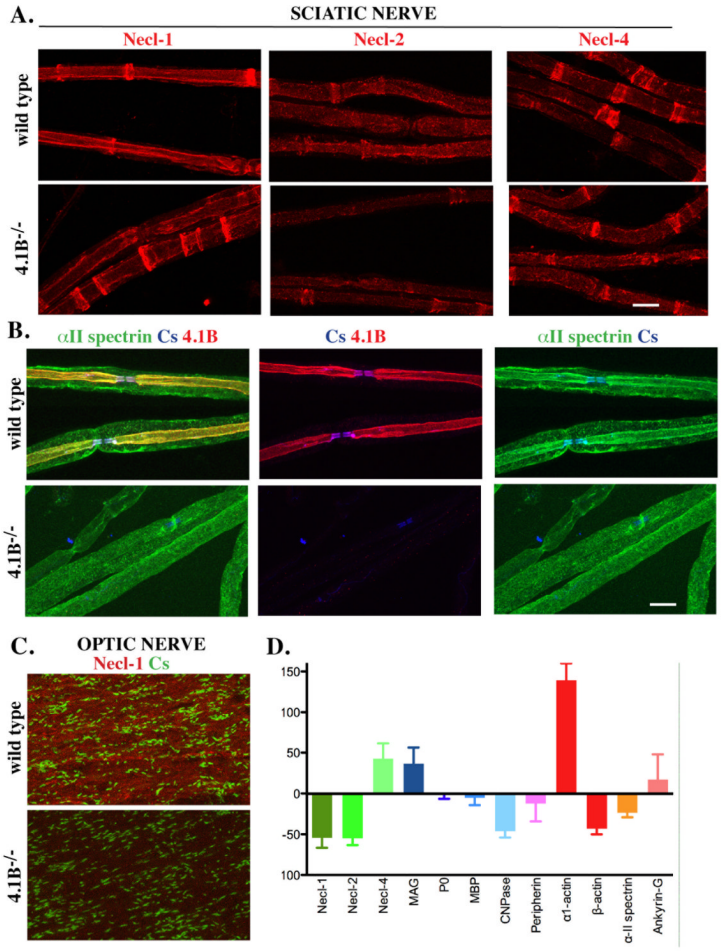

Figure 5. The expression of internodal components are altered in 4.1B$^{-/-}$ nerves

A. Teased sciatic nerves from wild type and *4.1B*$^{-/-}$ mice were stained for the Nectin-like proteins. There is a modest reduction of Necl-1 and Necl-2 along the internode but not the clefts; Necl-4 levels are largely unchanged. B. α2 spectrin staining co-localized with 4.1B along the internode of sciatic nerve fibers in wild type mice (yellow in the merged image). The inner staining that colocalizes with 4.1B along the axon was markedly reduced in the *4.1B*$^{-/-}$ nerves. C. A reduction of Necl-1 staining was observed in the optic nerve of the *4.1B*$^{-/-}$ mice although individual axons were not readily visualized. D. Summary of Western blotting data analyzing expression of myelin proteins, domain components and cytoskeletal proteins from three sets of sciatic nerves; the levels of these proteins in *4.1B*$^{-/-}$ mice are shown normalized to their levels in wild type mice. Scale bars (A, B) 10 μm.

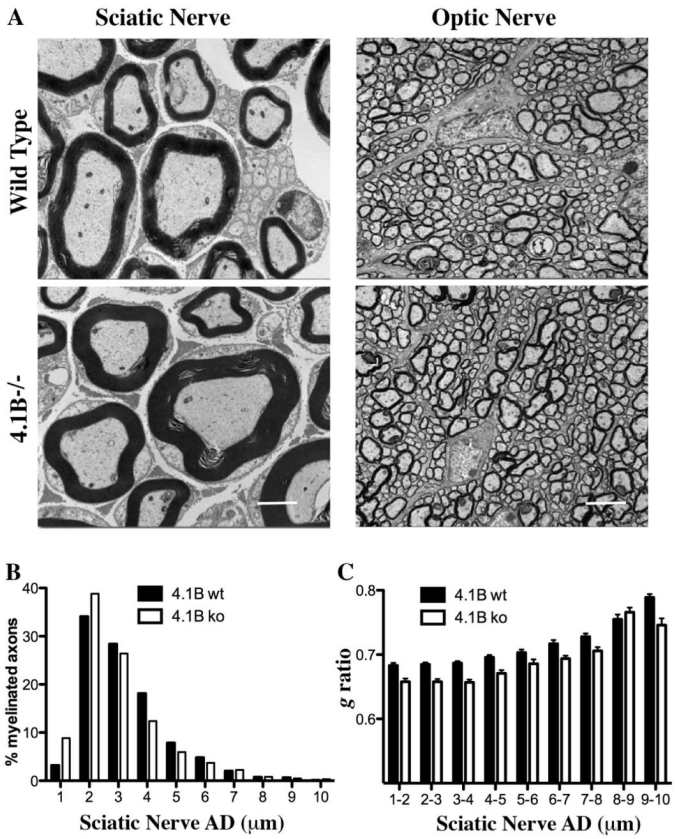

Figure 6. Ultrastructural analysis of myelinated axons in 4.1B$^{-/-}$ mice

A. EMs of sciatic and optic nerve cross-sections from wild type and *4.1B*$^{-/-}$ mice are shown; scale bars 2 μm (sciatic) and 4 μm (optic) nerve sections. B. Distribution of the percentage of myelinated fibers for each axon diameter is shown for wild type and *4.1B*$^{-/-}$ mice; there is an increase in the numbers of axons of smaller diameter (1 – 2 μm) that are myelinated in the 4.1B$^{-/-}$ mice C. Comparisons of the *g* ratios for myelinated sciatic nerve fibers binned for different axon diameters (AD); at every diameter, there is a reduction in the *g* ratios in the *4.1B*$^{-/-}$ mice.

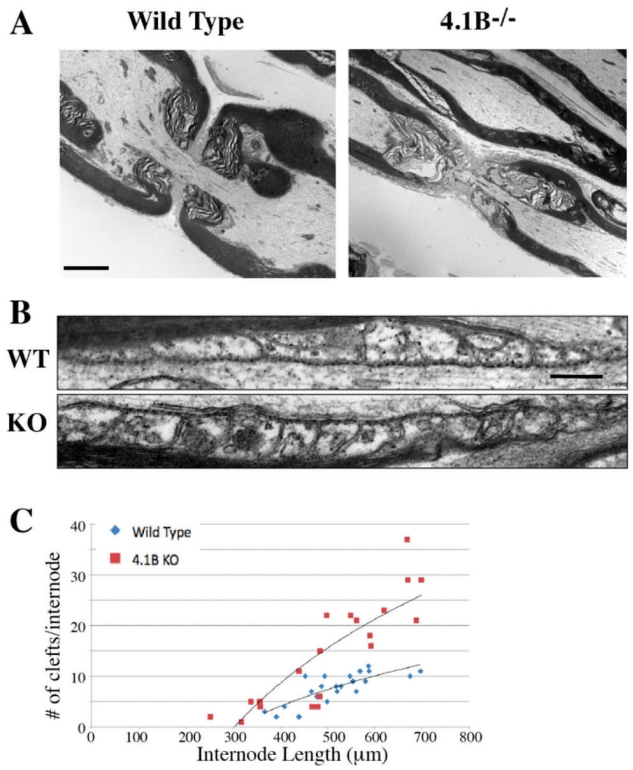

Figure 7. Organization of the nodal region and cleft numbers in 4.1B mutants

A. EMs of sciatic nerve fibers from wild type and *4.1B*$^{-/-}$ mice highlighting the longitudinal organization of the nodal regions are shown; scale bar, 4 μm. B. High power images through the optic nerve showing the organization of the paranodes demonstrate preservation of the close apposition of the paranodal loops and the presence of transverse bands in wild type (top) and *4.1B*$^{-/-}$ (bottom) optic nerves; scale bar, 200 nm. C. Quantitation of the numbers of Schmidt-Lanterman incisures as a function of internode length. *4.1B*$^{-/-}$ mutant nerves have approximately twice as many incisures per unit of length as do wt mice

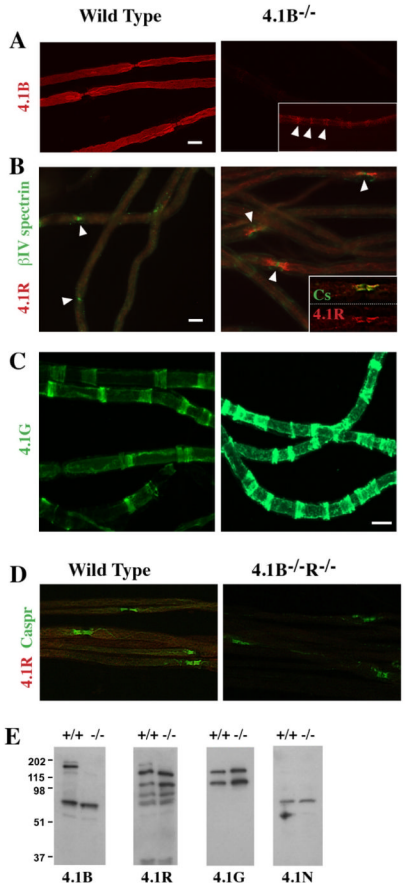

Figure 8. Compensatory changes by 4.1 proteins in the mutant nerves

Teased nerve fibers from wild type and *4.1B*$^{-/-}$ sciatic nerves were immunostained and blotted with a panel of antibodies to 4.1B, 4.1R and 4.1G. A. Staining with the 4.1B (HP) antibody demonstrates high-level expression along the axonal membrane, which is lost in the *4.1B*$^{-/-}$ sciatic nerves (the nerve fibers in the right panel are not visible on comparable exposure). On prolonged exposures (5X) of the mutant nerves (inset, right panel), persistent 4.1B staining is evident in the incisures, several of which are highlighted with arrowheads. B. 4.1R staining is undetected in wild type nerves but modestly increased in the paranodes of the *4.1B*$^{-/-}$ nerves; nodes are indicated by white arrowheads. The inset (right panel) shows staining of 4.1R overlaps substantially with that of Caspr in the paranodes. C. Nerves from the knockout mice exhibit increased numbers of incisures for fibers of the same diameter. In addition, staining for 4.1G appears increased in individual clefts. D. Caspr staining persists in the paranodes of the double *4.1B*$^{-/-}$ *4.1R*$^{-/-}$ sciatic nerves nerves. E. Blotting analysis of 4.1 proteins in wt vs. *4.1B*$^{-/-}$ sciatic nerves is shown; antibodies used were generated against the head piece (HP) of 4.1B, exon 19 of 4.1R, the U3 domain of 4.1G, and the HP of 4.1N (see Kang et al., 2009 for details). All scale bars, 10 μm.

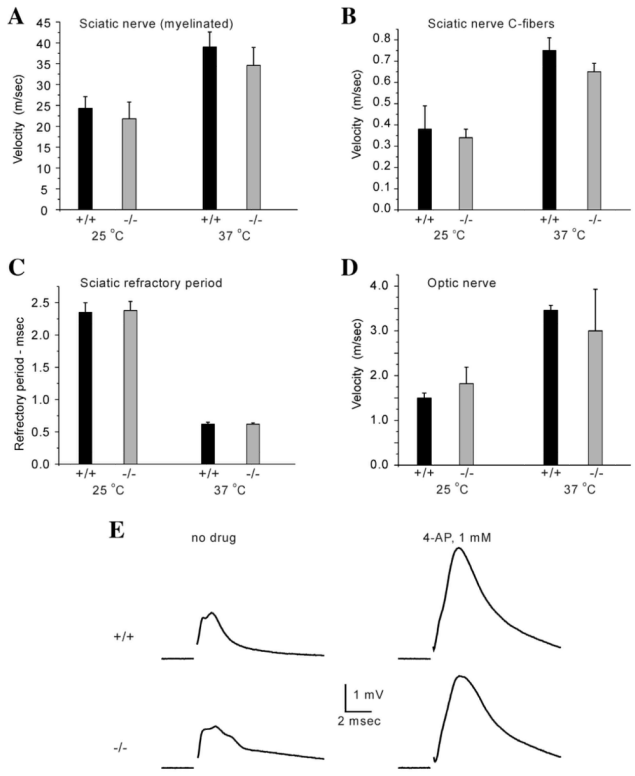

Figure 9. Electrophysiological Studies

Electrophysiological studies were carried out at room temperature and at 37° C on sciatic and optic nerves from wild type and *4.1B*$^{-/-}$ mice. A. Conduction velocity of myelinated axons in the sciatic nerve. B. Conduction velocity of unmyelinated C-fibers in the sciatic nerve. C. Refractory period of myelinated axons, sciatic nerve. D. Conduction velocity of optic nerves. E. Representative traces from optic nerves before and after exposure to 1 mM 4-aminopyridine (all at 37° C). The small gap in each record denotes the stimulus artifact.